Atomically Thin MoS$_2$: A New Direct-Gap Semiconductor

Kin Fai Mak,[1] Changgu Lee,[2] James Hone,[3] Jie Shan,[4] and Tony F. Heinz[1,*]

[1]*Departments of Physics and Electrical Engineering, Columbia University, 538 West 120th Street,
New York, New York 10027, USA*
[2]*SKKU Advanced Institute of Nanotechnology (SAINT) and Department of Mechanical Engineering,
Sungkyunkwan University, Suwon 440-746, Korea*
[3]*Department of Mechanical Engineering, Columbia University, New York, New York 10027, USA*
[4]*Department of Physics, Case Western Reserve University, 10900 Euclid Avenue, Cleveland, Ohio 44106, USA*

The electronic properties of ultrathin crystals of molybdenum disulfide consisting of $N = 1, 2, \ldots, 6$ S-Mo-S monolayers have been investigated by optical spectroscopy. Through characterization by absorption, photoluminescence, and photoconductivity spectroscopy, we trace the effect of quantum confinement on the material's electronic structure. With decreasing thickness, the indirect band gap, which lies below the direct gap in the bulk material, shifts upwards in energy by more than 0.6 eV. This leads to a crossover to a direct-gap material in the limit of the single monolayer. Unlike the bulk material, the MoS$_2$ monolayer emits light strongly. The freestanding monolayer exhibits an increase in luminescence quantum efficiency by more than a factor of 10^4 compared with the bulk material.

The transition-metal dichalcogenide semiconductor MoS$_2$ has attracted great interest because of its distinctive electronic, optical, and catalytic properties, as well as its importance for dry lubrication [1–19]. The bulk MoS$_2$ crystal, an indirect-gap semiconductor with a band gap of 1.29 eV [20], is built up of van der Waals bonded S-Mo-S units [2,5,6,11]. Each of these stable units (referred to as a MoS$_2$ monolayer) consists of two hexagonal planes of S atoms and an intermediate hexagonal plane of Mo atoms coordinated through ionic-covalent interactions with the S atoms in a trigonal prismatic arrangement (Fig. 1). Because of the relatively weak interactions between these layers and the strong intralayer interactions, the formation of ultrathin crystals of MoS$_2$ by the micromechanical cleavage technique is possible, as demonstrated by Novoselov *et al.* [21].

In this Letter, we report a systematic study of the evolution of the optical properties and electronic structure of ultrathin MoS$_2$ crystals as a function of layer number $N = 1, 2, 3, \ldots, 6$. We have investigated samples prepared both on solid surfaces and as freestanding films, entirely unperturbed by substrate interactions. The properties of the films were examined by using three complementary spectroscopic techniques: optical absorption, photoluminescence (PL), and photoconductivity, with additional sample characterization provided by atomic-force microscopy. The combination of these spectroscopic methods allowed us to trace the evolution of both the indirect and direct band gaps of the material as a function of layer thickness N. With decreasing N, the experiments reveal a progressive confinement-induced shift in the indirect gap from the bulk value of 1.29 eV to over 1.90 eV [22]. The change in the indirect-gap energy was found to be significantly larger than that of the direct gap, which increased by only 0.1 eV.

As a consequence of these different scaling properties and as suggested by previous calculations [8,9], the MoS$_2$ crystals exhibit a crossover from an indirect- to a direct-gap semiconductor in the monolayer limit. In addition to the signatures of this effect in the absorption and photoconductivity spectra, the PL quantum yield (QY) showed a dramatic enhancement in going from the dark, indirect-gap bulk crystal to the bright, direct-gap monolayer [23]. For our suspended samples, we observed an increase of the PL QY by more than a factor of 10^4 for the monolayer compared with the bulk crystal.

We prepared mono- and few-layer MoS$_2$ samples from bulk MoS$_2$ (SPI Supplies) by using a mechanical exfoliation technique similar to that employed for graphene [21]. Typical samples ranged from 25 to 200 μm^2 in size. Suspended samples were obtained by depositing the
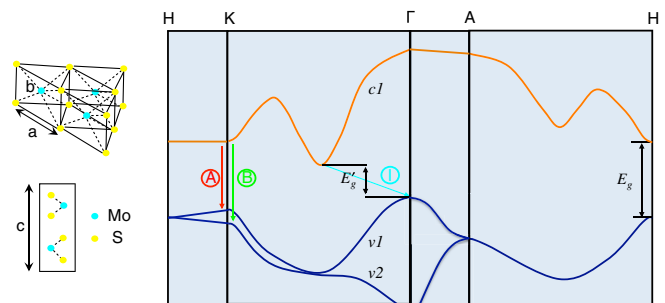

FIG. 1 (color online). Lattice structure of MoS$_2$ in both the in- and out-of-plane directions and simplified band structure of bulk MoS$_2$, showing the lowest conduction band $c1$ and the highest split valence bands $v1$ and $v2$. A and B are the direct-gap transitions, and I is the indirect-gap transition. E'_g is the indirect gap for the bulk, and E_g is the direct gap for the monolayer.

MoS_2 layers on oxide-covered Si substrates that had been prepared with arrays of holes (1.0 and 1.5 μm in diameter) [24]. We identified areas with thin MoS_2 samples with an optical microscope [Fig. 2(a)]. PL images were also collected to assess sample quality [Fig. 2(b)]. The reflectance contrast of the samples permits determination of their thickness with monolayer accuracy, as confirmed by atomic-force microscopy.

Optical measurements by absorption, PL, and photoconductivity spectroscopy were performed on mono- and few-layer MoS_2 samples. All optical measurements were carried out under ambient conditions at room temperature by using an inverted microscope (Nikon) coupled to a grating spectrometer with a CCD camera. The optical beams were focused on the sample with a spot diameter of $\sim$1 μm. For absorption measurements [25], samples on transparent fused quartz substrates were studied in the photon energy range of 1.3–3.0 eV by using a quartz-tungsten-halogen source. For PL studies, suspended samples were excited with a cw solid-state laser at a wavelength of 532 nm. A low laser power of $\sim$50 μW (on the sample) was used to avoid heating and PL saturation [26]. The PL QY of MoS_2 samples was calibrated by using rhodamine 6G molecules as the standard. For the photoconductivity studies, we prepared field-effect transistors of mono- and bilayer MoS_2 on silicon substrates covered by a 300-nm-thick oxide layer. Optical radiation of a well-defined frequency was selected from a supercontinuum laser source with a monochromator and was modulated with a mechanical chopper. The synchronous signal was detected with a lock-in amplifier [27].

As an indirect-gap material, band-gap PL in bulk MoS_2 is a weak phonon-assisted process and is known to have negligible QY. Appreciable PL was, however, observed from few-layer MoS_2 samples, and surprisingly bright PL was detected from monolayer samples. The measured PL intensity under identical excitation at 2.33 eV for a suspended monolayer and a bilayer sample is strikingly different [Fig. 3(a)]. The PL QY drops steadily with increasing thickness $N = 1$–6 [Fig. 3(a), inset]. A PL QY on the order

of 10^{-5}–10^{-6} was estimated for few-layer samples of $N = 2$–6; a value as high as 4×10^{-3} was observed in the limit of monolayer thickness. In addition to the significant difference in the PL QY, the normalized PL spectra for mono- and few-layer samples are quite distinct from one another [Fig. 3(b)]. The PL spectrum of suspended monolayer samples consists of a single narrow feature of $\sim$50 meV width, centered at 1.90 eV. In contrast, few-layer samples display multiple emission peaks (labeled A, B, and I). Peak A coincides with the monolayer emission peak. It shifts to the red and broadens slightly with increasing N. Peak B lies about 150 meV above peak A. The broad feature I, which lies below peak A, systematically shifts to lower energies, approaching the indirect-gap energy of 1.29 eV, and becomes less prominent with increasing N [Fig. 3(c)].

To understand the origin of these extraordinary PL properties, we compare the PL to the absorption spectrum of MoS_2. In the spectral range of 1.3–2.4 eV, absorption of bulk MoS_2 is dominated by two prominent transitions. They are known to arise from direct-gap transitions between the maxima of split valence bands ($v1$ and $v2$) and the minimum of the conduction band ($c1$), all located at the K point of the Brillouin zone (Fig. 1) [7,12–18]. The splitting arises from the combined effect of interlayer coupling and spin-orbit coupling. (The latter is not included in the band structure of Fig. 1 for simplicity.) The absorption spectrum of atomically thin layers of MoS_2 (normalized for thickness) was found to be largely unaltered, except for a slight blueshift of the resonances [Fig. 4(a)]. The monolayer PL peak A at 1.90 eV matches the lower absorption resonance in both its position and width. Therefore, we attribute the PL of monolayer MoS_2 to direct-gap luminescence. The result, combined with the high PL QY, also demonstrates the high quality of the suspended monolayer samples. For bilayer samples, on the other hand, emission peaks A and B match the two absorption resonances and are assigned to direct-gap hot luminescence [27]. The weak feature between A and B could be impurity or defect luminescence and merits further investigation. The PL peak I at 1.59 eV ($\sim$ 300 meV below the direct-gap absorption peak), as we discuss below, is attributed to indirect-gap luminescence.

Probing of the indirect-gap optical transitions in atomically thin layers of MoS_2 is limited by the sensitivity of absorption measurements. In the case of weak exciton binding, as for MoS_2 at room temperature, the photoconductivity spectrum mimics the absorption spectrum. Therefore, we used photoconductivity spectroscopy to investigate the optical response below the direct gap of mono- and bilayer MoS_2 [12]. The photoconductivity spectra of these samples could be recorded with signals ranging over three decades in strength [Fig. 4(b)]. For bilayer MoS_2, the onset of photoconductivity occurs around 1.60 eV, coinciding with the PL peak I. The conductivity increases slowly with photon energy towards the direct band gap, as expected for an indirect-gap material. In contrast, for monolayer MoS_2, the photoconductivity near 1.8 eV increases
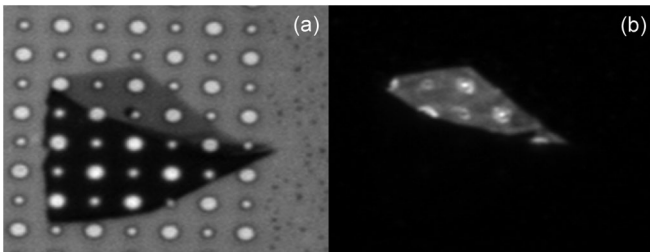

FIG. 2. (a) Representative optical image of mono- and few-layer MoS_2 crystals on a silicon substrate with etched holes of 1.0 and 1.5 μm in diameter. (b) PL image of the same samples. The PL QY is much enhanced for suspended regions of the monolayer samples, and the emission from the few-layer sample is too weak to be seen in this image.
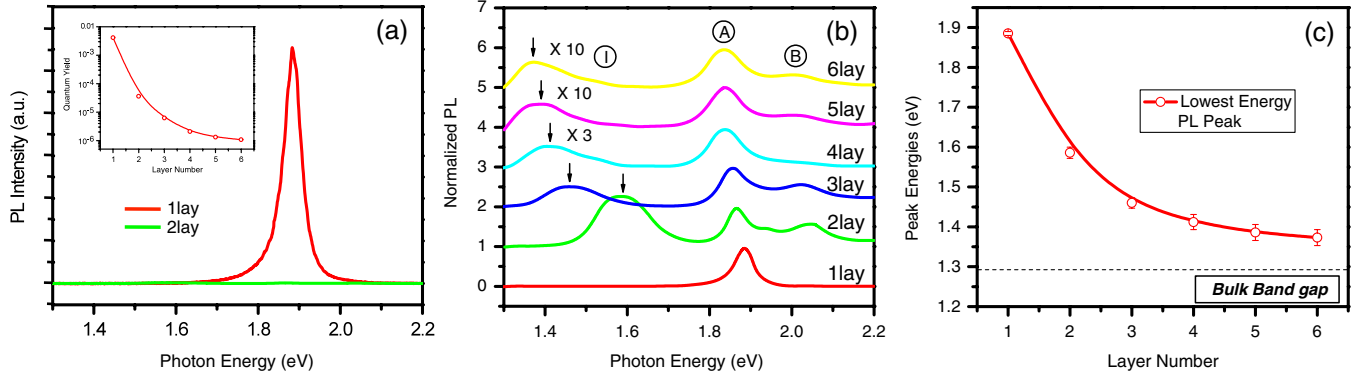
FIG. 3 (color online).   (a) PL spectra for mono- and bilayer MoS_2 samples in the photon energy range from 1.3 to 2.2 eV. Inset: PL QY of thin layers for $N = 1$–6. (b) Normalized PL spectra by the intensity of peak A of thin layers of MoS_2 for $N = 1$–6. Feature I for $N = 4$–6 is magnified and the spectra are displaced for clarity. (c) Band-gap energy of thin layers of MoS_2, inferred from the energy of the PL feature I for $N = 2$–6 and from the energy of the PL peak A for $N = 1$. The dashed line represents the (indirect) band-gap energy of bulk MoS_2.

(from a negligible value) by about 3 orders of magnitude. This dramatic rise corresponds to the onset of optical absorption from the direct band edge [28].

In the following simplified treatment of the spectral dependence of the photoconductivity, we neglect both excitonic effects and the variation of matrix elements with energy, factors that should be included in a more comprehensive theory. The absorbance $A(\hbar\omega)$ at photon energy $\hbar\omega$ near a direct band edge of energy E_g is then determined by the joint density of states. For a two-dimensional (2D) material like our atomically thin layers of MoS_2, this is described by a *step function*, $\Theta(\hbar\omega - E_g)$ [1,29]. After including a phenomenological broadening of 30 meV to account for finite temperature and scattering rates, we find that the photoconductivity spectrum of the monolayer samples can be fit well to this simple model [Fig. 4(b)]. This indicates that monolayer MoS_2 is indeed a direct-gap material [28]. On the other hand, the photoconductivity spectrum for bilayer MoS_2 cannot be described by the

step-function response. We need to include the effect of an indirect transition. Near an indirect band edge, the corresponding absorbance can be represented by [1,29]
$$A(\hbar\omega) \propto \sum_\alpha \left[\frac{\hbar\omega - \hbar\Omega_\alpha - E'_g}{1 - \exp(-\hbar\Omega_\alpha/kT)} + \frac{\hbar\omega + \hbar\Omega_\alpha - E'_g}{\exp(\hbar\Omega_\alpha/kT) - 1} \right] \propto \hbar\omega - E'_g.$$
Here E'_g and $\hbar\Omega_\alpha$ denote, respectively, the indirect-gap energy and that of the αth phonon mode, and kT is the thermal energy. By taking this term into account, the experimental bilayer MoS_2 spectrum can be fit well by an indirect transition at 1.6 eV, combined with a direct transition at 1.88 eV [Fig. 4(b)].

The indirect-direct-gap crossover as a function of MoS_2 thickness N is the result of a significant upshift of E'_g induced by perpendicular quantum confinement. To understand this, let us examine the electronic band structure of bulk MoS_2 (Fig. 1). The direct gap of ~1.8 eV occurs between $c1$ and $v1$ at the K point of the Brillouin zone (transitions A) [3–5,7,12]. On the other hand, the maximum of $v1$ and minimum of $c1$ are located at the Γ point and
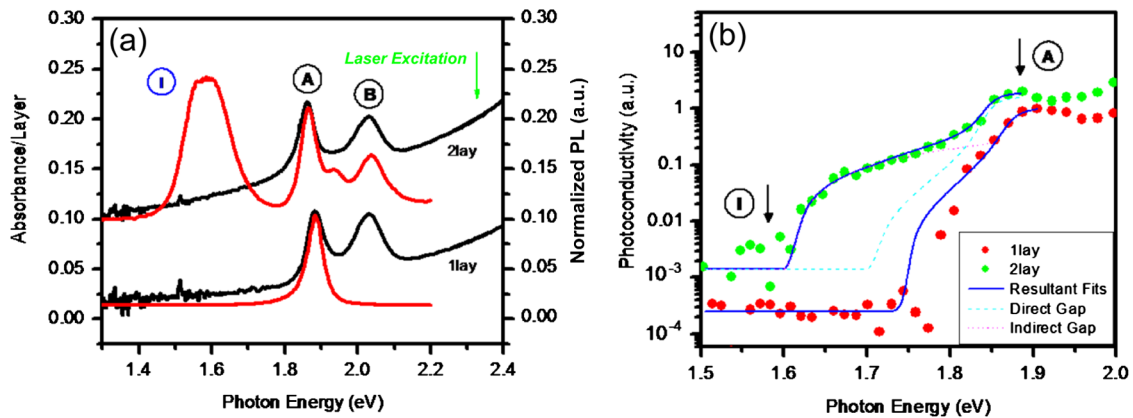

FIG. 4 (color online).   (a) Absorption spectra (left axis, normalized by N) and the corresponding PL spectra (right axis, normalized by the intensity of the peak A). The spectra are displaced along the vertical axis for clarity. (b) Photoconductivity spectra for mono- (red dots) and bilayer (green dots) samples [27]. The data are compared with the 2D model described in the text (blue lines). E_g and E'_g inferred from the PL measurements, indicated by arrows, are included for comparison.

along the Γ-K direction [3–6,8,11], respectively; they form an indirect gap of 1.29 eV (transition I) [20]. The out-of-plane mass $m_\perp$ for electrons and holes around the K point far exceeds the free electron mass m_0; on the other hand, $m_\perp$ for holes around the Γ point is estimated to be $\sim 0.4m_0$ and for electrons around the $c1$ minimum along the Γ-K direction to be $\sim 0.6m_0$. Thus, while decreasing N leads to a large confinement-induced increase in the indirect gap E'_g, the direct gap E_g remains almost unchanged. The indirect-direct-gap crossover is reached in the limit of monolayer thickness.

To explain this result more precisely, we apply a zone-folding scheme to describe the electronic states of the ultrathin samples [30,31]. For identical layers with only nearest-neighbor interlayer interactions, the 2D electronic structure of few-layer MoS_2 samples can be generated as a subset of the bulk electronic states with quantized out-of-plane momenta $k_\perp$, i.e., momenta lying in planes perpendicular to the Γ-A or K-H directions. For monolayer MoS_2, the allowed plane passes directly through the H and A points. The $c1$ minimum and the $v1$ maximum of the resulting 2D bands both occur at the H point (Fig. 1). Monolayer MoS_2 therefore becomes a direct-gap material. With increasing N, cuts with $k_\perp$ approaching the Γ-K line are made. Then the $v1$ maximum and the $c1$ minimum occur at the Γ point and along the Γ-K direction, respectively, as in the bulk material. Few-layer MoS_2 samples are, therefore, indirect-gap semiconductors. These findings agree with earlier *ab initio* calculations of few-layer MoS_2 [8,9]. Our result is distinct from zone-folding-induced pseudodirect transitions in semiconductor superlattice structures [32], which have very low oscillator strength and PL QY.

The crossover from an indirect-gap material to a direct-gap material naturally accounts for the more than 10^4-fold enhancement of the luminescence QY observed in monolayer MoS_2. It is consistent with the observed absorption spectra that show little sensitivity to the layer number N and a band gap that decreases with increasing N. The observed dependence of the band gap on N is also in qualitative agreement with published density-functional theory calculations [8]. Monolayer MoS_2 constitutes the first atomically thin material that is an effective emitter of light. Its strong PL suggests its use for photostable markers and sensors that can be adapted to probe nanoscale dimensions. The controllability of the band gap may also be used to optimize the material's use as a photocatalytic agent [19] and for photovoltaic applications. Our results highlight that the distinctive electronic properties of atomically thin layered materials are not restricted to graphene but extend to a broader group of van der Waals bonded solids.

*Corresponding author.
tony.heinz@columbia.edu

[1] P. A. Lee, *Physics and Chemistry of Materials with Layered Structures: Optical and Electrical Properties* (Reidel, Dordrecht, 1976).
[2] R. A. Bromley, A. D. Yoffe, and R. B. Murray, J. Phys. C **5**, 759 (1972).
[3] R. V. Kasowski, Phys. Rev. Lett. **30**, 1175 (1973).
[4] L. F. Mattheis, Phys. Rev. Lett. **30**, 784 (1973).
[5] L. F. Mattheis, Phys. Rev. B **8**, 3719 (1973).
[6] R. Coehoorn et al., Phys. Rev. B **35**, 6195 (1987).
[7] R. Coehoorn, C. Haas, and R. A. Degroot, Phys. Rev. B **35**, 6203 (1987).
[8] T. S. Li and G. L. Galli, J. Phys. Chem. C **111**, 16 192 (2007).
[9] S. Lebegue and O. Eriksson, Phys. Rev. B **79**, 115409 (2009).
[10] J. C. McMenamin and W. E. Spicer, Phys. Rev. B **16**, 5474 (1977).
[11] T. Boker et al., Phys. Rev. B **64**, 235305 (2001).
[12] K. K. Kam and B. A. Parkinson, J. Phys. Chem. **86**, 463 (1982).
[13] B. L. Evans and P. A. Young, Proc. R. Soc. A **284**, 402 (1965).
[14] B. L. Evans and P. A. Young, Proc. Phys. Soc. London **91**, 475 (1967).
[15] J. A. Wilson and A. D. Yoffe, Adv. Phys. **18**, 193 (1969).
[16] A. R. Beal, W. Y. Liang, and J. C. Knights, J. Phys. C **5**, 3540 (1972).
[17] W. Y. Liang, J. Phys. C **6**, 551 (1973).
[18] A. R. Beal and H. P. Hughes, J. Phys. C **12**, 881 (1979).
[19] X. Zong et al., J. Am. Chem. Soc. **130**, 7176 (2008).
[20] *Gmelin Handbook of Inorganic and Organometallic Chemistry* (Springer-Verlag, Berlin, 1995), 8th ed., Vol. B7.
[21] K. S. Novoselov et al., Proc. Natl. Acad. Sci. U.S.A. **102**, 10 451 (2005).
[22] Changes in the phonon spectra as a function of the layer thickness of MoS_2 have also been observed by using Raman spectroscopy: C. Lee et al., ACS Nano **4**, 2695 (2010).
[23] Enhancement of PL QY in the MoS_2 monolayer samples has recently been reported in an independent study: A. Splendiani et al., Nano Lett. **10**, 1271 (2010).
[24] C. Lee, X. D. Wei, J. W. Kysar, and J. Hone, Science **321**, 385 (2008); S. P. Berciaud, S. Ryu, L. E. Brus, and T. F. Heinz, Nano Lett. **9**, 346 (2009).
[25] K. F. Mak et al., Phys. Rev. Lett. **101**, 196405 (2008).
[26] M. Virsek, M. Krause, A. Kolitsch, and M. Remskar, Phys. Status Solidi B **246**, 2782 (2009).
[27] See supplementary material at http://link.aps.org/supplemental/10.1103/PhysRevLett.105.136805 for details about the sample preparation, characterization, and optical measurement techniques, as well as assignment of the PL features.
[28] The indirect-to-direct band-gap crossover is determined with a resolution on the order of the thermal energy $kT \sim 26$ meV.
[29] C. Hamaguchi, *Basic Semiconductor Physics* (Springer-Verlag, Berlin, 2001).
[30] M. Koshino and T. Ando, Phys. Rev. B **76**, 085425 (2007).
[31] K. F. Mak, M. Y. Sfeir, J. A. Misewich, and T. F. Heinz, Proc. Natl. Acad. Sci. U.S.A. **107**, 14 999 (2010).
[32] H. Presting et al., Semicond. Sci. Technol. **7**, 1127 (1992).